Neuron, Vol. 42, 23–36, April 8, 2004, Copyright ©2004 by Cell Press

Loss of Presenilin Function Causes Impairments of Memory and Synaptic Plasticity Followed by Age-Dependent Neurodegeneration

Carlos A. Saura,[1] Se-Young Choi,[2] Vassilios Beglopoulos,[1] Seema Malkani,[1] Dawei Zhang,[1,2] B.S. Shankaranarayana Rao,[3] Sumantra Chattarji,[3] Raymond J. Kelleher III,[4] Eric R. Kandel,[5] Karen Duff,[6] Alfredo Kirkwood,[2] and Jie Shen[1,*]

[1]Center for Neurologic Diseases
Brigham and Women's Hospital
Program in Neuroscience
Harvard Medical School
Boston, Massachusetts 02115
[2]Mind/Brain Institute
Johns Hopkins University
Baltimore, Maryland 21218
[3]National Centre for Biological Sciences
Bangalore 560065
India
[4]The Picower Center for Learning and Memory
Massachusetts Institute of Technology
Cambridge, Massachusetts 02139
[5]Howard Hughes Medical Institute
Center for Neurobiology and Behavior
Columbia University
New York, New York 10032
[6]Nathan Kline Institute
Orangeburg, New York 10962

Summary

Mutations in presenilins are the major cause of familial Alzheimer's disease, but the pathogenic mechanism by which presenilin mutations cause memory loss and neurodegeneration remains unclear. Here we demonstrate that conditional double knockout mice lacking both presenilins in the postnatal forebrain exhibit impairments in hippocampal memory and synaptic plasticity. These deficits are associated with specific reductions in NMDA receptor-mediated responses and synaptic levels of NMDA receptors and αCaMKII. Furthermore, loss of presenilins causes reduced expression of CBP and CREB/CBP target genes, such as *c-fos* and *BDNF*. With increasing age, mutant mice develop striking neurodegeneration of the cerebral cortex and worsening impairments of memory and synaptic function. Neurodegeneration is accompanied by increased levels of the Cdk5 activator p25 and hyperphosphorylated tau. These results define essential roles and molecular targets of presenilins in synaptic plasticity, learning and memory, and neuronal survival in the adult cerebral cortex.

Introduction

Alzheimer's disease is an age-related neurodegenerative illness characterized clinically by progressive deterioration of memory and other cognitive abilities and neuropathologically by progressive loss of neurons and synapses and by the formation of amyloid plaques and neurofibrillary tangles. Dominantly inherited mutations in presenilins 1 and 2 are the primary cause of familial Alzheimer's disease (FAD) (Hutton and Hardy, 1997). The pathogenic mechanism by which presenilin mutations cause memory loss and neurodegeneration, however, remains unclear.

Presenilins (PS) are integral components of a multiprotein protease complex, termed γ-secretase, which is responsible for the intramembranous cleavage of the amyloid precursor protein (APP) and the Notch receptors (De Strooper et al., 1998, 1999). FAD-linked PS mutations selectively enhance production of the amyloidogenic 42-residue β-amyloid (Aβ) peptide, often at the expense of the less amyloidogenic Aβ40 generation (Moehlmann et al., 2002; Schroeter et al., 2003), suggesting a toxic gain-of-function pathogenic mechanism. However, FAD-linked *PS1* alleles have a reduced ability to rescue the mutant phenotypes of *sel-12*, a functional *PS1* homolog in *C. elegans* (Baumeister et al., 1997; Levitan et al., 1996). In mammalian cells, mutant forms of PS1 produce reduced levels of the intracellular domains of Notch and APP, which can function as transcriptional activators (Cao and Sudhof, 2001; Moehlmann et al., 2002; Schroeter et al., 2003; Song et al., 1999). Furthermore, FAD-linked PS1 mutations include exonic deletions (Crook et al., 1998; Tysoe et al., 1998) and more than 140 distinct missense mutations distributed throughout the coding sequence rather than clustered in a specific functional domain(s), consistent with a partial loss-of-function mechanism. These findings raise the possibility that partial loss of normal presenilin function may underlie disease processes. Due to the early embryonic lethality of $PS^{-/-}$ mice (Donoviel et al., 1999), the normal physiological role of presenilins in the adult brain, however, is not yet known.

Neuropathological studies have indicated that synaptic abnormalities may represent the proximate cause of dementia in AD. Synapse loss provides a better correlate of the pattern and severity of cognitive impairment than amyloid plaques or neurofibrillary tangles (Terry et al., 1991). In addition, synaptic and dendritic loss precede frank neuronal loss and are most prominent in limbic regions corresponding to the clinical deficits (Braak and Braak, 1997; Terry et al., 1991). Abnormalities in learning and synaptic function have been observed in APP transgenic mice as a consequence of elevated Aβ levels (Hsia et al., 1999; Hsiao et al., 1996), but the molecular mechanisms by which increased production of Aβ affects learning and synaptic function have not been defined.

Intensive studies of the mechanisms underlying hippocampal long-term potentiation (LTP) and memory formation have delineated central roles for NMDA receptors, calcium/calmodulin-dependent kinase II (CaMKII), and cAMP response element (CRE)-dependent gene expression, which is mediated by the transcription factor CREB (CRE binding protein) and the coactivator CREB binding protein (CBP) (Kandel, 2001; Lonze and Ginty, 2002). Several molecules that play key roles in LTP and

*Correspondence: jshen@rics.bwh.harvard.edu

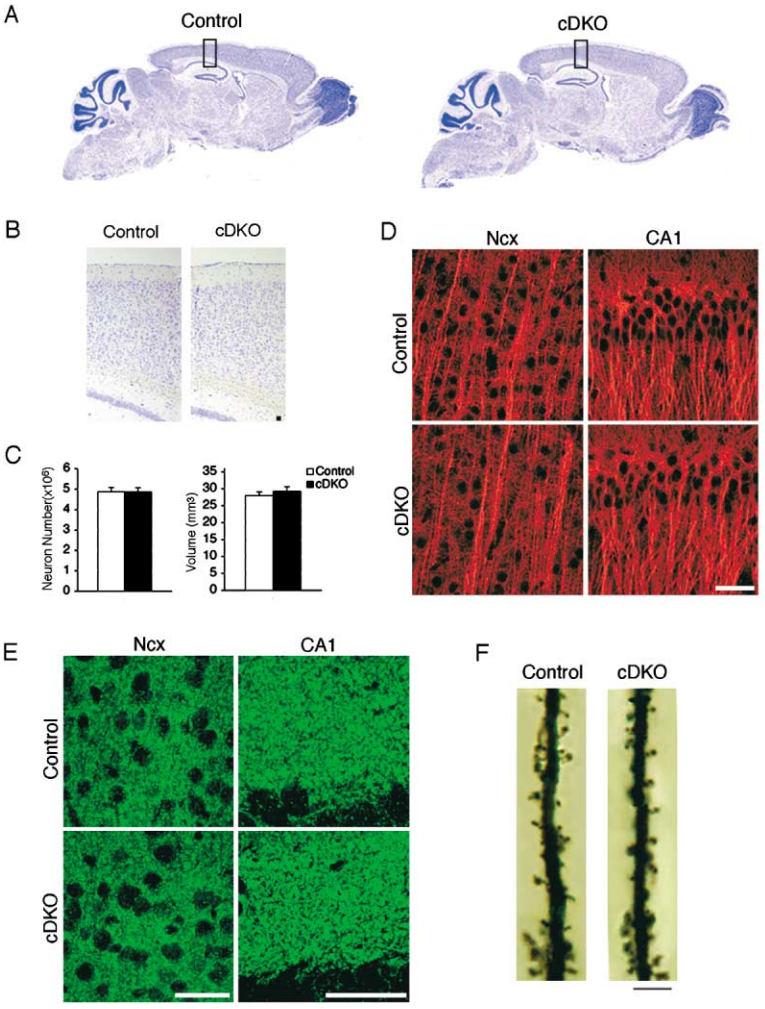

Figure 1. Normal Brain Morphology of *PS* cDKO Mice at 2 Months of Age

(A) Normal brain cytoarchitecture revealed by Nissl staining of comparable sagittal sections of *PS* cDKO and control brains.

(B) Higher magnification views of the boxed areas in (A).

(C) Normal neuron number and volume in the neocortex of *PS* cDKO mice (n = 4) relative to control mice (n = 5).

(D and E) Similar MAP2 (D) and synaptophysin (E) immunoreactivity in the neocortex (Ncx) and hippocampal area CA1 (CA1) of *PS* cDKO and control brains. Scale bar equals 50 μm.

(F) Golgi impregnation of CA1 pyramidal neurons reveals similar spine density in *PS* cDKO and control dendrites. Scale bar equals 2.5 μm.

memory, such as BDNF and CREB, have also been implicated in neuronal survival. The intriguing finding that inactivation of CREB and the related modulatory factor CREM in the postnatal forebrain causes striking neurodegeneration provides support for a mechanistic link between synaptic plasticity and neuronal survival (Mantamadiotis et al., 2002). Further, reduced CBP function, leading to reduced CRE-dependent gene expression, has been implicated in the pathogenesis of neurodegeneration in polyglutamine repeat disorders (Nucifora et al., 2001). It remains unclear, however, whether the genetic defects in FAD impinge upon the central mechanisms underlying LTP and memory.

Our previous investigation of normal presenilin function revealed an essential role of PS1 in neurogenesis and the Notch signaling pathway (Handler et al., 2000; Shen et al., 1997). To extend this study to the adult cerebral cortex, which is the most relevant experimental system for the investigation of AD pathogenesis, we generated a viable *PS1* conditional knockout (cKO), in which expression of PS1 is selectively eliminated in excitatory neurons of the forebrain beginning at postnatal day ~18 (Yu et al., 2001). This hypomorphic *PS* mutant mouse exhibits normal hippocampal synaptic transmission and plasticity and a subtle deficit in spatial memory (Yu et al., 2001). To overcome the early embryonic lethality of $PS^{-/-}$ mice so as to investigate PS function in the adult brain, we generated conditional *PS* null mice lacking both PS1 and PS2 in the postnatal forebrain. These mice exhibit impairments in hippocampal memory and LTP prior to any neuropathological changes, demonstrating a requirement for PS in normal synaptic plasticity. More specifically, we found a selective reduction in NMDA receptor-mediated responses and synaptic levels of NMDA receptors and αCaMKII in mutant mice. Furthermore, in the absence of PS, levels of CBP and transcription of CREB/CBP target genes are reduced. Strikingly, *PS* cDKO mice subsequently develop in an age-dependent manner synaptic, dendritic, and neuronal degeneration with accompanying astrogliosis and hyperphosphorylation of tau, demonstrating an essential role for PS in neuronal survival.

Results

Normal Brain Morphology in *PS* cDKO Mice at 2 Months

To generate forebrain-specific *PS* conditional double knockout (*PS* cDKO) mice, we crossed floxed *PS1* (*fPS1*), *αCaMKII-Cre* transgenic (Yu et al., 2001), and $PS2^{-/-}$

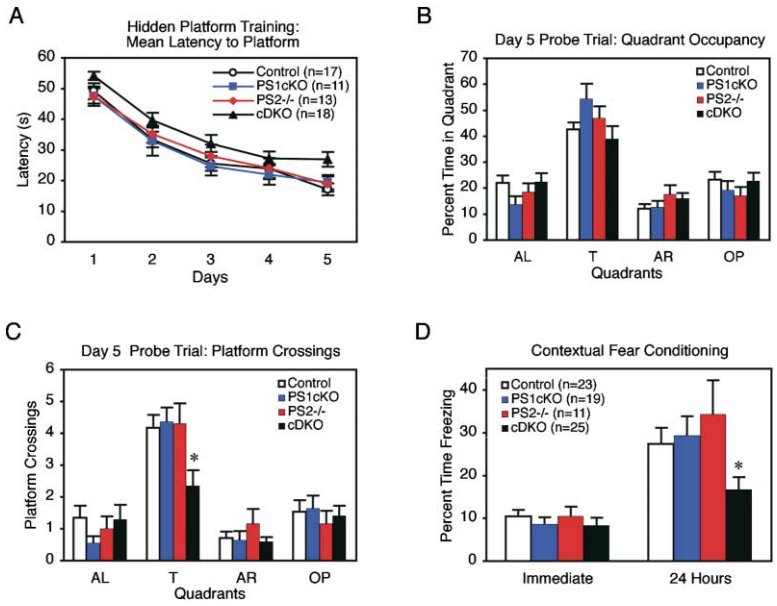

Figure 2. Impaired Spatial and Associative Memory in *PS* cDKO Mice at 2 Months of Age

(A) Longer escape latencies in *PS* cDKO mice. On training day 5, *PS* cDKO mice (26.9 ± 2.4) display significantly longer latencies compared to control mice (17.1 ± 1.9; $p < 0.005$).

(B) All four genotypic groups show a preference for the target quadrant [T versus AL, AR, OP; $p < 0.0002$) (group × quadrant interaction, $F(9,216) = 2.18$; $p < 0.03$]. AL, adjacent left; T, target quadrant; AR, adjacent right; OP, opposite quadrant.

(C) Significantly reduced platform crossings in *PS* cDKO mice compared to control mice ($p < 0.0003$) [group × quadrant interaction, $F(9,216) = 2.26$; $p < 0.02$].

(D) In contextual fear conditioning, all four genotypic groups show indistinguishable levels of freezing immediately after footshock ($p > 0.62$). *PS* cDKO mice show significantly reduced levels of freezing compared to control ($p < 0.01$) at 24 hr posttraining.

The number of mice used in each experiment is indicated in parentheses.

(Steiner et al., 1999) mice together to obtain *fPS1/fPS1;* αCaMKII-Cre;*PS2*$^{-/-}$ mice. In situ hybridization and Western analyses confirmed progressive inactivation of PS1 and absence of PS2 in the cortex of cDKO mice (data not shown). During early adulthood, *PS* cDKO mice are viable and indistinguishable from littermate controls. Open field and rotarod tests of *PS* cDKO mice at 2–3 months of age revealed no significant alterations in general behavior, motor coordination, and exploratory anxiety (data not shown).

At 2 months of age, Nissl-stained brain sections of *PS* cDKO, *PS1* cKO, *PS2*$^{-/-}$, and control mice revealed similar brain morphology (Figures 1A and 1B, data not shown). Stereological analysis of *PS* cDKO ($n = 4$) and control ($n = 5$) brains demonstrated similar neuronal number and neocortical volume ($p > 0.05$) (Figure 1C). Immunoreactivity for microtubule-associated protein 2 (MAP2) and synaptophysin in the neocortex and hippocampus was similar for all four genotypes (Figures 1D and 1E, data not shown). Golgi-stained pyramidal neurons in hippocampal area CA1 displayed similar dendritic spine morphology and density in *PS* cDKO and control mice (Figure 1F). Together, these results indicate normal brain cytoarchitecture, neuronal number, and morphology in *PS* cDKO mice at this age.

Mild Memory Impairment in *PS* cDKO Mice at 2 Months

To determine the functional effects of PS inactivation in the adult brain, we examined hippocampal learning and memory in *PS* cDKO mice using the Morris water maze task. The performance of all four genotypic groups improved significantly during the course of training (day 1 versus day 5, $p < 0.0001$) (Figure 2A). *PS* cDKO mice, however, exhibited significantly longer latencies ($p < 0.001$) and path lengths ($p < 0.0001$) relative to the control group, while their swimming speed was similar ($p = 0.23$) (Figure 2A, data not shown). In the posttraining probe trial, all four genotypic groups searched preferentially in the target quadrant ($p < 0.0002$) (Figure 2B). The total number of platform crossings by *PS* cDKO mice (2.4 ± 0.5), however, was significantly lower than that of control mice (4.2 ± 0.4), *PS1* cKO (4.4 ± 0.4), and *PS2*$^{-/-}$ (4.3 ± 0.6) mice ($p < 0.0003$) (Figure 2C). To determine whether the memory impairment exhibited by *PS* cDKO mice could be due to poor vision, motivation, and/or sensorimotor abilities, all four genotypic groups were tested in the visible platform task with 4 trials per day for 5 days. All groups improved their performance rapidly with similarly low latencies ($p > 0.5$) (data not shown). These results demonstrate that *PS* cDKO mice exhibit a mild but detectable impairment in spatial memory.

We next assessed all four genotypic groups in contextual fear conditioning, in which robust hippocampal memory can be acquired in a single trial. All four genotypic groups displayed similar levels of freezing immediately after training ($p > 0.62$). When presented with the training context after a retention delay of 24 hr, however, *PS* cDKO mice (16.7% ± 2.8%) showed significantly reduced levels of freezing compared to control (27.4% ± 3.7%), *PS1* cKO (29.4% ± 4.4%), and *PS2*$^{-/-}$ (34.3% ± 7.7%) mice ($p < 0.01$) (Figure 2D). These results show that long-term contextual memory is intact in *PS1* cKO and *PS2*$^{-/-}$ mice but impaired in cDKO mice.

Impaired Synaptic Plasticity in *PS* cDKO Mice at 2 Months

The cognitive deficits exhibited by *PS* cDKO mice prompted us to investigate whether presenilins are required for the modulation of synaptic function. We examined the Schaeffer collateral pathway of *PS* cDKO mice for deficits in synaptic transmission and two forms of plasticity, long-term potentiation (LTP) and long-term depression (LTD). We first quantified the initial slope of the evoked field excitatory postsynaptic potential (fEPSP) and the amplitude of the fiber volley (FV), which is a measure of the number of recruited axons, in acute hippocampal

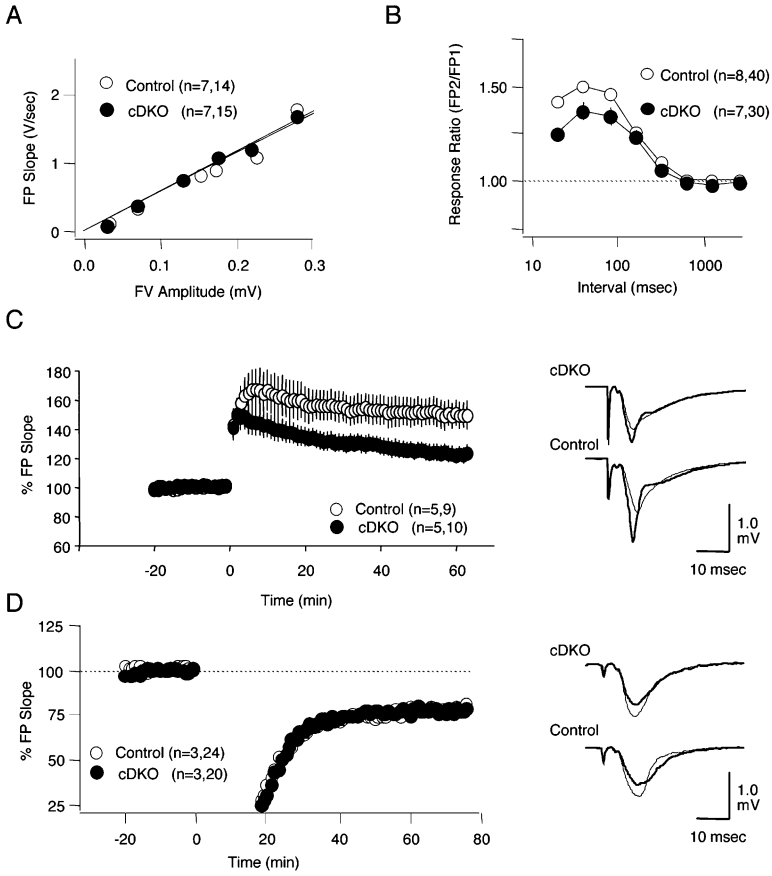

Figure 3. Impaired Synaptic Plasticity in *PS* cDKO Mice at 2 Months of Age

(A) Normal synaptic transmission in *PS* cDKO mice [$t(10) = 13.30$, $p < 0.001$]. The synaptic input-output relationship was obtained by plotting the fiber volley amplitude against the initial slope of the evoked fEPSP. Each point represents data averaged across all slices for a narrow bin of FV amplitude. The lines represent the best linear regression fit (*PS* cDKO: $y = 5.35x$, $R^2 = 0.940$; control: $y = 6.55x$, $R^2 = 0.933$).

(B) Reduced PPF in *PS* cDKO mice [$F(7,476) = 5.67$, $p < 0.0001$]. The graph depicts the paired-pulse response ratio (2^{nd} fEPSP/1^{st} fEPSP) obtained at different interstimulus intervals (in ms).

(C) Impaired LTP in *PS* cDKO mice. Left: Time course of the effects of 5 TBS on the fEPSP initial slope. Repeated measures ANOVA analysis of the magnitude of LTP in *PS* cDKO and control mice shows an interaction effect between group and time [$F(9,288) = 2.9$, $p < 0.002$]. Right: Examples of induced LTP. Superimposed traces are averages of four consecutive responses 1 min before (thin line) and 60 min after (thick line) TBS.

(D) Normal LTD in *PS* cDKO mice. Left: Time course of the effects of ppLFS on the fEPSP initial slope [$F(9,153) = 1.43$, $p = 0.18$]. Right: Superimposed traces are recorded 1 min before (thin line) and 60 min after (thick line) ppLFS.

The number of mice (left) and slices (right) used in each experiment is indicated in parentheses.

slices. In *PS* cDKO mice, the maximal fEPSP (2.86 ± 0.21 V/s) and FV (0.59 ± 0.07 mV) were normal compared to control mice (2.50 ± 0.21 V/s, $p = 0.46$ for fEPSP; 0.52 ± 0.04 mV, $p = 0.32$ for FV). Input/output (I/O) curves, which were obtained by plotting the amplitude of FV versus the fEPSP slope, were similar in *PS* cDKO and control mice ($p = 0.32$), indicating normal basal synaptic transmission (Figure 3A). Paired-pulse facilitation (PPF), a presynaptic form of short-term plasticity, was significantly reduced in *PS* cDKO mice ($p < 0.0001$), suggesting an increase in the probability of neurotransmitter release (Figure 3B).

We next explored the effects of presenilin inactivation on synaptic plasticity. LTP induced by 5 trains of theta burst stimulation (TBS) was reduced in *PS* cDKO mice (Figure 3C). The magnitude of LTP measured 60 min after TBS in *PS* cDKO mice (121.6% ± 4.5%) was significantly lower relative to control mice (150.9% ± 8.8%, $p < 0.002$). LTD induced by a paired-pulse low-frequency stimulation (ppLFS), which has been shown to induce LTD effectively in slices of mature mice (Kemp and Bashir, 1997), was unaffected in *PS* cDKO mice (Figure 3D). The magnitude of LTD measured 75 min after conditioning in *PS* cDKO mice (81.3% ± 1.7%) was similar to that in control mice (78.0% ± 1.9%; $p = 0.23$). Thus, inactivation of presenilins selectively compromises LTP but not LTD. Together, these results show that presenilins are required for normal synaptic plasticity, providing a cellular basis for the memory deficits observed in *PS* cDKO mice.

Selective Reductions in NMDA Receptor Function and Synaptic αCaMKII Levels

NMDA receptors play a key role in the induction of LTP (Bliss and Collingridge, 1993). We therefore explored the possibility that changes in the synaptic responses mediated by NMDA receptors might underlie the LTP deficit in *PS* cDKO mice. We first quantified the ratio of NMDA receptor (NMDAR)-mediated to AMPA receptor (AMPAR)-mediated responses recorded under voltage clamp in CA1 pyramidal neurons. As shown in Figure 4A, the NMDAR/AMPAR ratio was greatly diminished in *PS* cDKO mice (0.11 ± 0.02) compared to control mice (0.29 ± 0.05, $p < 0.0004$), whereas AMPAR amplitude was similar in both genotypes ($p = 0.77$). The decrease in the NMDAR/AMPAR ratio suggests a decrease in NMDAR response, since the I/O curve, which measures primarily the AMPAR response, is normal in *PS* cDKO mice (Figure 3A). To measure NMDAR responses more directly, we isolated NMDAR-mediated responses pharmacologically and normalized them to the FV amplitude. Again, we found a dramatic reduction in the NMDAR/FV ratio in *PS* cDKO mice ($p < 0.001$) (Figure 4B), indicating a severe reduction of postsynaptic NMDAR-mediated responses in these mutant mice at 2 months of age.

To explore the mechanism underlying reduced NMDAR responses further, we measured the levels of NMDAR subunits in the cerebral cortex of *PS* cDKO and control mice at 2 months of age. Western analysis showed that total cortical levels of NR1, NR2A, and NR2B subunits were unchanged. However, the levels of NR1 and NR2A

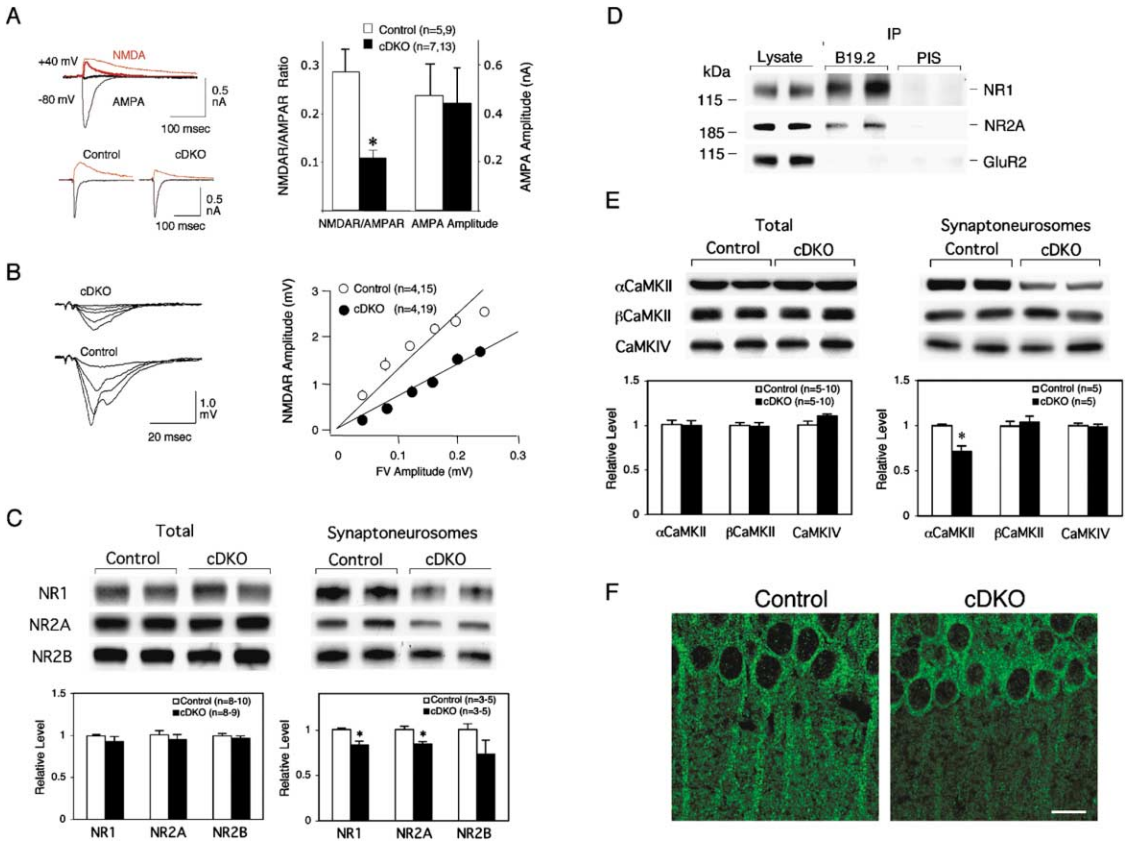

Figure 4. Reduced NMDAR Responses and Reduced Synaptic NMDAR and αCaMKII Levels in *PS* cDKO Mice at 2 Months of Age

(A) NMDAR- and AMPAR-mediated responses recorded under voltage clamp. Left: Representative current traces recorded at +40 mV (thin red trace) and −80 mV (thin black trace) from *PS* cDKO and control CA1 pyramidal neurons. APV (100 μM) blocks the late component of the currents recorded at +40 mV (thick red trace), while CNQX (10 μM) eliminates the currents recorded at −80 mV (thick black trace). Right: Reduced NMDAR/AMPAR ratio ($p < 0.0004$) and unchanged AMPAR amplitude ($p = 0.77$) in *PS* cDKO mice.

(B) Left: Representative field responses evoked by varying stimulation intensities in the presence of CNQX (10 μM) and BMI (10 μM) in *PS* cDKO and control hippocampal slices. Right: Reduction of the NMDAR-mediated responses, normalized to the fiber volley amplitude, in *PS* cDKO mice. The I/O slopes (*PS* cDKO: $y = 7.01x$, $R^2 = 0.992$; control: $y = 12.90x$, $R^2 = 0.967$) are significantly different ($p < 0.001$).

(C) Reduced synaptic levels of NR1 and NR2A in *PS* cDKO mice. Levels of NR1, NR2A, and NR2B are similar in cortical lysates of *PS* cDKO and control mice ($p > 0.26$). Levels of NR1 ($p < 0.005$) and NR2A ($p < 0.02$) are significantly reduced in cortical synaptoneurosomes prepared from *PS* cDKO mice.

(D) Specific interaction of PS1 and NMDARs in the cerebral cortex. Membrane extracts from cerebral cortex were immunoprecipitated using an anti-PS1 N-terminal antiserum (B19.2) or preimmune serum (PIS) followed by Western analysis using antibodies specific for NR1, NR2A, or GluR2.

(E) Reduced synaptic levels of αCaMKII in *PS* cDKO mice. Levels of αCaMKII, βCaMKII, and CaMKIV are unchanged in cortical lysates of *PS* cDKO mice, while levels of αCaMKII ($p < 0.001$) but not βCaMKII and CaMKIV are reduced in cortical synaptoneurosomes from *PS* cDKO mice.

(F) Confocal images show reduced dendritic αCaMKII immunoreactivity in hippocampal CA1 pyramidal neurons of *PS* cDKO mice. Scale bar equals 25 μm.

in synaptoneurosome preparations, which are enriched for synaptic proteins (Scheetz et al., 2000), were significantly reduced (Figure 4C). This reduction in synaptic levels of the major NMDAR subunits in the adult cerebral cortex may account for the impaired NMDAR responses in *PS* cDKO mice. These findings suggested the possibility that synaptic localization of NMDARs might be regulated through physical association with presenilins. To address this possibility, we performed co-immunoprecipitation experiments in cortical membrane fractions. Endogenous NR1 and NR2A co-immunoprecipitated specifically with PS1 (Figure 4D), providing support for the notion that normal synaptic delivery of NMDARs may require the formation of stable complexes with presenilins.

NMDAR-mediated responses are known to regulate the activity, synaptic levels, and localization of CaMKII, which plays a key role in synaptic plasticity (Lisman et al., 2002; Thiagarajan et al., 2002). We therefore examined levels of the α and β isoforms of CaMKII in the cerebral cortex of *PS* cDKO and control mice. Consistent with the defect in NMDAR responses, synaptic levels of αCaMKII were reduced in *PS* cDKO mice, while synaptic levels of βCaMKII and CaMKIV were unchanged (Figure 4E). Furthermore, αCaMKII immunoreactivity was lower in dendrites but not cell bodies of *PS* cDKO hippocampal pyramidal neurons (Figure 4F). The selective reduction of synaptic and dendritic αCaMKII could further contribute to the impairments in synaptic plasticity, learning, and memory observed in *PS* cDKO mice.

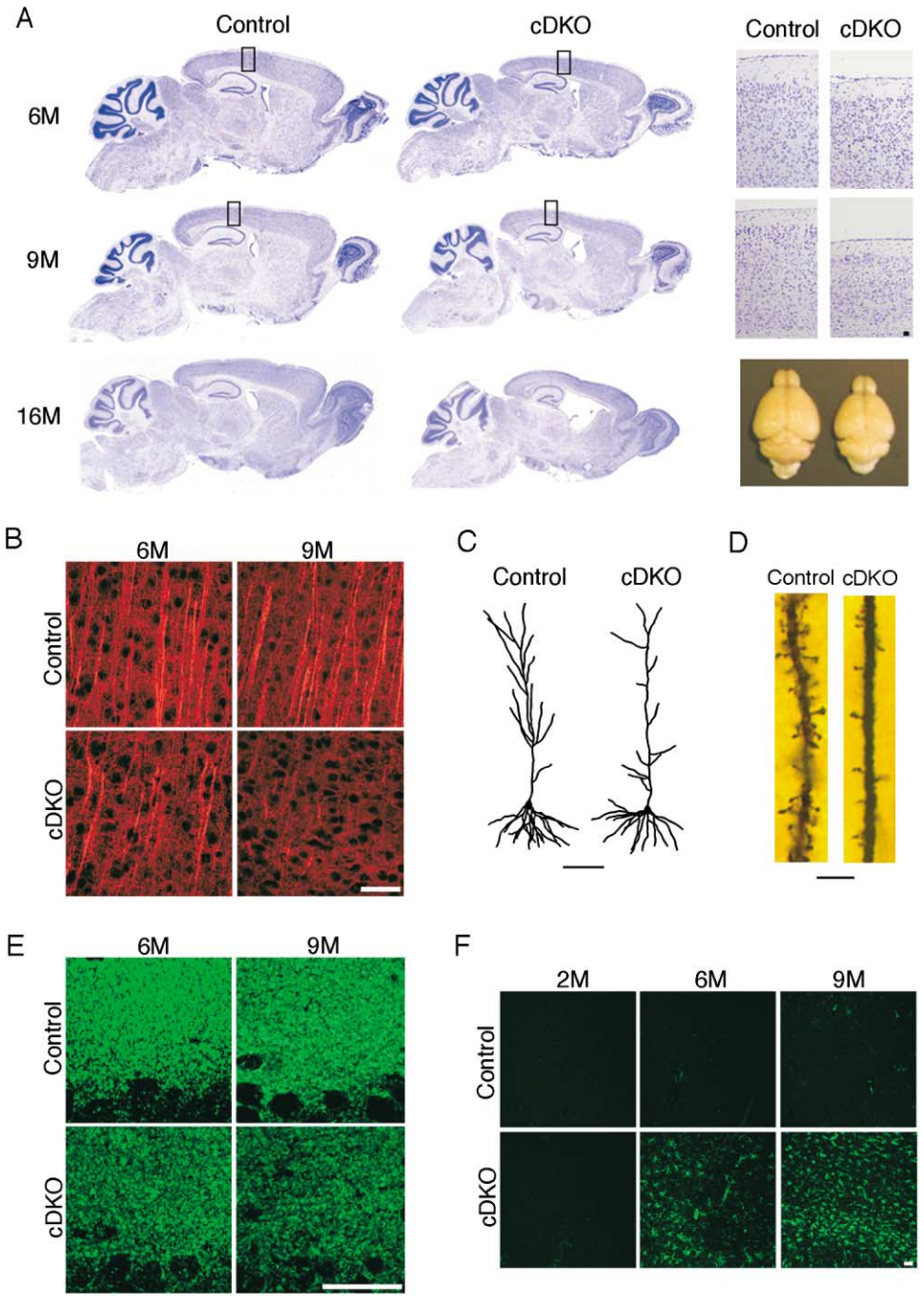

Figure 5. Progressive Neuronal Degeneration in *PS* cDKO Mice

(A) Left: Nissl staining of comparable sagittal sections of *PS* cDKO and control brains at 6, 9, and 16 months (M) of age demonstrates progressive loss of gray and white matter in the neocortex and hippocampus and enlargement of lateral ventricles. Right: Higher-magnification views of the neocortex show progressive thinning of cortical layers at 6 and 9 months of age. By 16 months of age, gross cerebral atrophy is evident in *PS* cDKO mice.

(B) Progressive reduction in MAP2 immunoreactivity in the neocortex of *PS* cDKO mice at 6 and 9 months of age.

(C) Camera lucida drawing shows reduced dendritic complexity of Golgi-impregnated CA1 pyramidal neurons in *PS* cDKO mice at 9 months of age.

(D) Loss of dendritic spines in Golgi-impregnated CA1 pyramidal neurons of *PS* cDKO mice at 9 months of age.

(E) Reduced synaptophysin immunoreactivity in hippocampal area CA1 of *PS* cDKO mice at 6 and 9 months of age.

(F) Progressive and striking astrogliosis as indicated by increased GFAP immunoreactivity in the neocortex of *PS* cDKO mice at 6 and 9 months of age.

Scale bar equals 50 μm in (A)–(C), (E), and (F) and 2.5 μm in (D).

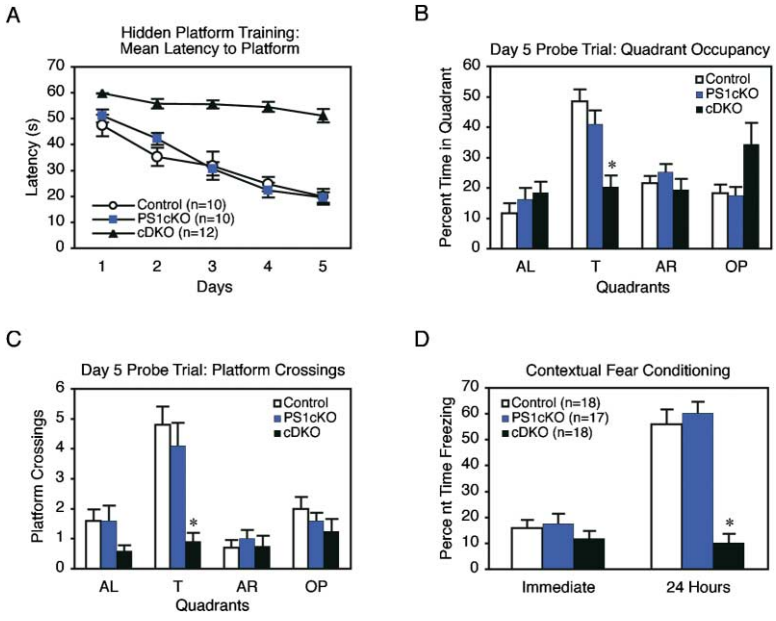

Figure 6. Severely Impaired Spatial and Associative Memory in *PS* cDKO Mice at 6 Months of Age

(A) Longer escape latencies in *PS* cDKO mice. On training day 5, control (19.9 ± 3.1) and *PS1* cKO (19.6 ± 2.1) mice display significantly shorter latencies compared to *PS* cDKO mice (51.2 ± 2.5, $p < 0.0001$).

(B) During the probe trial on day 5, control (48.5 ± 3.9) and *PS1* cKO (41.0 ± 4.6) mice display a preference for the target quadrant (T versus AL, AR, OP; $p < 0.0001$), whereas *PS* cDKO mice spend similar amounts of time in all quadrants ($p > 0.05$) [group × quadrant interaction, $F(6,116) = 6.96$; $p < 0.0001$]. AL, adjacent left; T, target quadrant; AR, adjacent right; OP, opposite quadrant.

(C) Control and *PS1* cKO mice cross the platform location significantly more frequently than *PS* cDKO mice [group × quadrant interaction, $F(6,116) = 5.14$; $p < 0.0001$].

(D) In contextual fear conditioning, *PS* cDKO, *PS1* cKO, and control mice display indistinguishable levels of freezing immediately after footshock [$F(2,50) = 0.9$; $p = 0.41$]. *PS* cDKO mice (10.1 ± 3.4) exhibit reduced levels of freezing compared to control ($p < 0.0001$) and *PS1* cKO ($p < 0.0001$) mice at 24 hr posttraining [$F(2,50) = 38.7$; $p < 0.0001$]. The number of mice per genotype used in each experiment is indicated in parentheses.

Age-Dependent Neuronal Degeneration in *PS*cDKO Mice

To determine whether loss of PS function in the adult brain produces age-dependent anatomical alterations, we analyzed *PS* cDKO mice at 6, 9, and 16 months of age. These mutant mice begin to exhibit excessive grooming behavior, increased stereotypy in the open field, and reduced latency in the rotarod test at the age of 6 months (data not shown). Nissl-stained brain sections demonstrated progressive and striking loss of cerebral cortical gray and white matter accompanied by enlargement of the lateral ventricles (Figure 5A). Stereological quantification of neuronal number and volume of the neocortex of *PS* cDKO ($n = 7$) and control ($n = 7$) mice at 6–9 months of age demonstrated an 18%–24% reduction in neuronal number ($p < 0.05$) and ~35% reduction in neocortical volume ($p < 0.05$).

Immunohistochemical analysis revealed marked, progressive reduction in MAP2 reactivity in the neocortex (Figure 5B) and the hippocampus of *PS* cDKO mice at 6 and 9 months of age. Golgi staining demonstrated a reduction in the dendritic complexity and spine density of CA1 pyramidal neurons (Figures 5C and 5D). Quantification of CA1 pyramidal neurons ($n = 40$ for cDKO; $n = 30$ for control) of *PS* cDKO ($n = 4$) and control ($n = 3$) brains revealed a 25% reduction in the total length of dendrites ($p < 0.0005$) and 15% and 11% decreases in branch points of apical ($p < 0.001$) and basal ($p < 0.02$) dendrites, respectively. Synaptophysin immunoreactivity was also markedly reduced in the hippocampus (Figure 5E) and neocortex, indicating loss of presynaptic terminals. The loss of neurons, dendrites, and presynaptic terminals was accompanied by an age-dependent inflammatory response, as indicated by a dramatic increase in astrogliosis with age in the neocortex (Figure 5F) and hippocampus. Glial fibrillary acidic protein (GFAP) immunoreactivity was absent at 2 months but became progressively more severe at 6 and 9 months of age. Collectively, these results document age-dependent, progressive neurodegeneration in mice lacking presenilins in the postnatal forebrain.

Severe Memory Impairment and Synaptic Dysfunction in *PS* cDKO Mice at 6 Months

To assess the impact of ongoing neuronal degeneration on learning and memory, we next tested *PS* cDKO, *PS1* cKO, and control mice at 6 months of age in the water maze task. *PS* cDKO mice performed very poorly, with significantly longer latencies and path lengths compared to control and *PS1* cKO mice ($p < 0.0001$), whereas *PS1* cKO mice performed as well as control mice with similar latencies ($p = 0.29$) (Figure 6A) and path lengths ($p = 0.84$). The posttraining probe trial revealed that *PS1* cKO and control mice displayed significantly higher occupancies of the target quadrant relative to other quadrants ($p < 0.0001$), whereas *PS* cDKO mice failed to show such a preference ($p > 0.05$) (Figure 6B). The number of platform crossings by *PS* cDKO mice (0.9 ± 0.3) was much lower than that of control (4.8 ± 0.6) and *PS1* cKO (4.1 ± 0.8) mice ($p < 0.0001$) (Figure 6C). Their swimming speed during the 5-day training period and their performance in the visible platform task were indistinguishable from control and *PS1* cKO groups ($p > 0.05$) (data not shown), indicating that the performance deficit of *PS* cDKO mice in the water maze was not due to impaired sensorimotor abilities. We further examined *PS* cDKO, *PS1* cKO, and control mice at 6 months of age in contextual fear conditioning. Although all three genotypic groups displayed similar levels of freezing immediately after training ($p = 0.41$), *PS* cDKO mice (10.2% ± 3.5%) showed significantly reduced levels of freezing when presented with the training context after a retention delay of 24 hr relative to control (56% ± 6%) and *PS1* cKO (60.2% ± 4.5%) mice

($p < 0.0001$) (Figure 6D). Consistent with the neurodegeneration documented by morphological analysis, these behavioral results together demonstrate significant progression of the memory impairments in *PS* cDKO mice between 2 and 6 months of age.

Since memory abilities markedly deteriorate in *PS* cDKO mice between 2 and 6 months of age, we further examined these mice at 6 months for deficits in synaptic transmission and plasticity in the Schaeffer collateral pathway. In *PS* cDKO mice, the maximal fEPSP was normal (2.0 ± 0.3 V/s) compared to control mice (2.3 ± 0.2, $p = 0.36$), but the maximal fiber volley was significantly reduced ($p < 0.02$) (Supplemental Figures S1A–S1C at http://www.neuron.org/cgi/content/full/42/1/23/DC1), indicating that fewer axons were recruited upon stimulation. Input/output curves were elevated in *PS* cDKO mice ($p < 0.001$), indicating enhanced basal synaptic transmission (Supplemental Figure S1D), which could represent a compensatory effect due to loss of presynaptic axonal terminals, as indicated by reduced synaptophysin immunoreactivity and FV amplitude in hippocampal CA1 synapses. PPF was significantly reduced in *PS* cDKO mice ($p < 0.0001$) (Supplemental Figure S1E). Further, LTP induced by 5 trains of TBS was reduced ($p < 0.002$), while LTD induced by paired-pulse low-frequency stimulation was unaffected ($p = 0.18$) in *PS* cDKO mice (Supplemental Figures S1F and S1G). Thus, despite ongoing neuronal degeneration, the effects of loss of presenilin function on synaptic plasticity remain specific for LTP.

Downregulation of CREB-Dependent Gene Expression

In addition to CaMKII, NMDAR-mediated responses also regulate CRE-dependent gene expression (Lonze and Ginty, 2002), which is essential for the long-lasting synaptic changes underlying long-term memory (Kandel, 2001). Further, conditional double knockout mice lacking CREB and its modulator CREM in the adult forebrain develop striking neuronal degeneration (Mantamadiotis et al., 2002). To determine whether deficient CRE-dependent gene expression could contribute to the synaptic plasticity impairments and neuronal degeneration observed in *PS* cDKO mice, we examined the expression of multiple CREB/CBP target genes. Quantitative real-time RT-PCR analysis of cerebral cortical RNA derived from 2-month-old mice ($n = 10$–11) revealed a significant decrease in expression of CREB/CBP target genes, including *c-fos* (51% reduction) and exon III-containing *BDNF* transcripts (64% reduction) (Figure 7A). Expression of exon III-containing *BDNF* transcripts is most responsive to neuronal and CREB/CBP activities compared to the more abundant transcripts expressed from promoters in exons I, II, and IV (Tao et al., 1998). Total levels of *BDNF* transcripts derived from all promoters were unchanged in *PS* cDKO mice (Figure 7A), confirming the specificity of the reduction in the exon III-containing transcripts. Similar results for multiple CREB/CBP-target genes were obtained at 5 weeks (1 week after PS1 is widely inactivated) and 6 months of age (after *PS* cDKO mice have lost 18% of cortical neurons) (data not shown). The levels of c-Fos protein were similarly reduced (57%) in *PS* cDKO mice (Figure 7B). These results demonstrate that presenilins positively regulate CRE-dependent transcription in the adult brain. Mutant mice lacking *c-fos* or BDNF have been shown to exhibit synaptic plasticity impairments and spatial memory deficits (Fleischmann et al., 2003; Korte et al., 1995; Patterson et al., 1996). Thus, downregulation of CRE-dependent gene expression may provide a molecular mechanism linking impaired synaptic plasticity with neurodegeneration in *PS* cDKO mice.

To determine the molecular mechanism underlying the observed reduction in CRE-dependent gene expression in *PS* cDKO mice, we measured nuclear levels of Ser133-phosphorylated CREB, total CREB, and CBP. Analysis of nuclear extracts prepared from the cerebral cortex of 2-month-old *PS* cDKO and control mice revealed similar levels of Ser133-phosphorylated and total CREB (Figure 7C). In contrast, nuclear levels of CBP were significantly reduced in *PS* cDKO mice ($p < 0.03$) (Figure 7D). Levels of total CBP (both nuclear and cytoplasmic) were similarly reduced ($p < 0.002$). Consistent with reduced levels of CBP protein, quantitative real-time RT-PCR analysis showed that the level of *CBP* transcripts was reduced in the cerebral cortex of *PS* cDKO mice at 2 months of age (Figure 7E). The magnitude of the measured CBP reduction likely represents an underestimate due to normal PS1 expression in nonexcitatory neurons and glia in *PS* cDKO mice. Furthermore, we found that the predicted *CBP* (*Crebbp*) promoter (NCBI: NT 039624) contains a consensus recognition site for the transcription factor CBF1 (also known as RBP-J_K) through which the active form of the Notch intracellular domain exerts its transcriptional activation effects. The sequences of the CBF1 binding site in the *CBP* promoter conform to the consensus sequences and are identical to the CBF1 binding sites of the canonical Notch/RBP-J_K downstream target genes, *Hes1* and *Hes5*, indicating that *CBP* is likely a downstream target gene of the Notch signaling pathway (Figure 7F).

Increased p25 Levels and Hyperphosphorylation of Tau in Older *PS* cDKO Mice

To determine whether neurodegeneration in *PS* cDKO mice is associated with hyperphosphorylation of tau, we examined control and *PS* cDKO mice at 9 months of age. Western analysis of cortical lysates using an anti-tau antibody specific for dephosphorylated serine 202 and threonine 205 (Tau 1) revealed a reduction of dephosphorylated tau in *PS* cDKO mice (Figure 8A). Western analysis using antibodies specific for phosphorylated serine 202 and threonine 205 (AT-8 and CP13), phosphorylated serines 396 and 404 (PHF-1), and phosphorylated threonine 231 (AT-180) showed an increase of phosphorylated tau in *PS* cDKO brains (Figure 8A). Furthermore, Western analysis of phosphatase-treated cortical lysates demonstrated similar total levels of tau isoforms in *PS* cDKO and control mice (Figure 8B), indicating that the heightened levels of phosphorylated tau detected in *PS* cDKO mice are due to hyperphosphorylation rather than any increase in total tau levels. Immunohistological analysis of *PS* cDKO brain sections using the CP13 antibody confirmed cytoplasmic accumulation of hyperphosphorylated tau in cerebral cortical neurons (data not shown).

Abnormal phosphorylation of tau in AD has been asso-

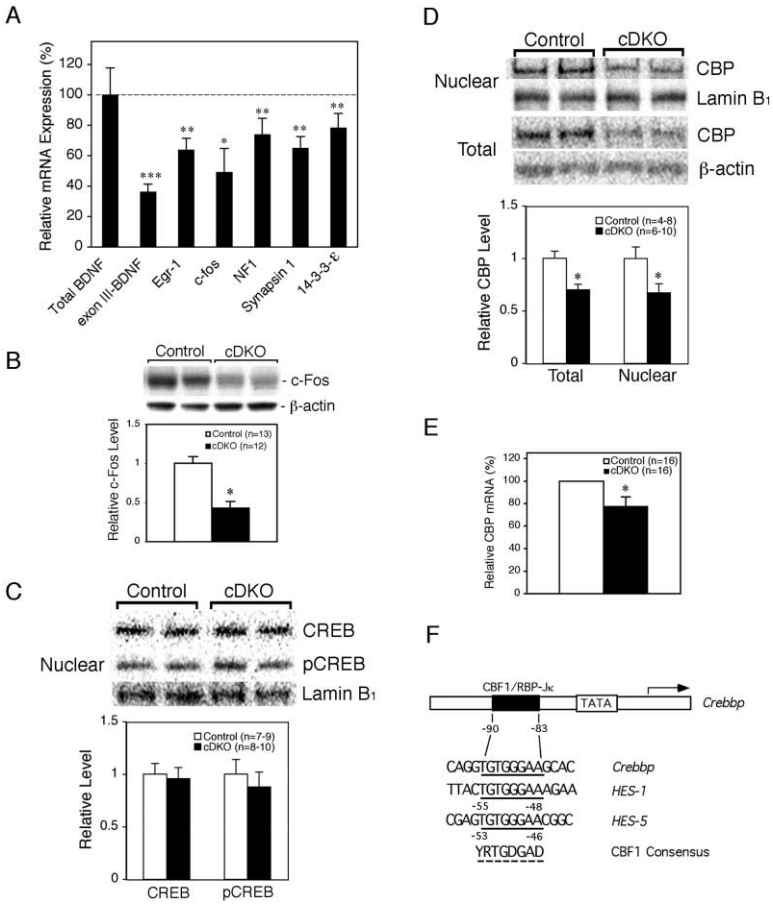

Figure 7. Reduced CBP and CREB/CBP-Dependent Gene Expression in *PS* cDKO Mice at 2 Months of Age

(A) Real-time RT-PCR analysis reveals reduced expression of CRE-dependent genes in *PS* cDKO mice. mRNA expression is expressed as percentage values of the control. *$p < 0.05$, **$p < 0.01$, ***$p < 0.0001$.

(B) Reduced levels of c-Fos in cerebral cortex of *PS* cDKO mice. Cortical lysates from *PS* cDKO and control mice were analyzed by Western analysis (top) with antibodies specific for c-Fos and β-actin. Results were quantified and c-Fos levels were normalized to β-actin levels (bottom).

(C) Normal levels of CREB and phospho-Ser133 CREB (pCREB) in *PS* cDKO mice. Western analysis (top) and quantification (bottom) show normal levels of CREB and phospho-Ser133 CREB in nuclear extracts from *PS* cDKO cerebral cortex. ^{125}I-labeled secondary antibodies were used, and bands were quantified by phosphorimaging. Values are normalized to levels of lamin B_1, a nuclear protein used as loading control.

(D) Reduced levels of CBP in *PS* cDKO mice. Western analysis (top) and quantification (bottom) show reduced levels of CBP in total ($p < 0.002$) and nuclear ($p < 0.03$) extracts from *PS* cDKO cerebral cortex. ^{125}I-labeled secondary antibodies were used, and results were quantified by phosphorimaging. Values are normalized to lamin B_1 or β-actin levels.

(E) Quantitative real-time RT-PCR analysis reveals reduced CBP mRNA levels in the cerebral cortex of *PS* cDKO mice (*$p < 0.03$). mRNA expression is expressed as a percentage of the control values.

(F) Sequences of the predicted CBF1/RBP-Jκ binding site in the *Crebbp (CBP)* proximal promoter. Scheme of the mouse *Crebbp* promoter showing the consensus CBF1/RBP-Jκ binding site (black box), the TATA box, and the predicted transcriptional start site (arrow). The CBF1/RBP-Jκ binding sequences from the proximal promoters of the canonical Notch target genes *HES-1* and *HES-5* (solid line) and the consensus recognition sequence (dashed line) are shown for comparison. The numbering is relative to the TATA box. Y = C/T, R = G/A, D = A/G/T.

ciated with upregulation of Cdk5 kinase activity as a consequence of p35 cleavage to generate the more potent activator p25 (Patrick et al., 1999). Interestingly, tau was hyperphosphorylated in *PS* cDKO mice at residues known to be phosphorylated by Cdk5 in vivo, which suggests that altered Cdk5 activity might be responsible for the observed tau hyperphosphorylation. We therefore examined the levels of Cdk5 and its activators p35 and p25 in cerebral cortical extracts. Western analysis showed similar levels of Cdk5 and p35 in *PS* cDKO and control mice at 2, 6, and 9 months of age, but levels of p25 were elevated in *PS* cDKO mice in an age-dependent manner with very low levels of p25 at 6 months and higher levels of p25 at 9 months (Figure 8C, data not shown). Thus, progressive accumulation of p25 and hyperphosphorylation of tau likely further contribute to the progressive neuronal degeneration observed in *PS* cDKO mice.

Discussion

Essential Role of Presenilins in Synaptic Plasticity

Presenilins are the major genes of familial Alzheimer's disease, but the early embryonic lethality of *PS* null mice precluded investigation of PS function in the adult brain, where the pathogenesis of AD takes place (Donoviel et al., 1999). To overcome this problem, we temporally and spatially restricted PS inactivation to excitatory neurons of the postnatal forebrain and thereby were able to investigate their role in the adult brain. Our behavioral analysis revealed that disruption of both presenilins causes impairments in hippocampal learning and memory. Electrophysiological analysis in the Schaeffer collateral pathway demonstrated that loss of presenilin function results in selective impairments in LTP and NMDAR-mediated synaptic responses, providing a cellular basis for memory impairments observed in these mutant mice. Importantly, these defects were evident at an age prior to the onset of any detectable neuropathological abnormalities. Furthermore, the selective impairments in hippocampal memory and LTP, with preservation of normal sensorimotor function, basal synaptic transmission, and LTD, argue against a global impairment of neuronal function. These results demonstrate that presenilins are required for synaptic plasticity and learning and memory in the adult brain.

Molecular Mechanisms of LTP and Memory Deficits Caused by Loss of PS Function

To characterize the molecular mechanism by which loss of PS function leads to impaired hippocampal LTP and memory, we focused on the molecules known to play

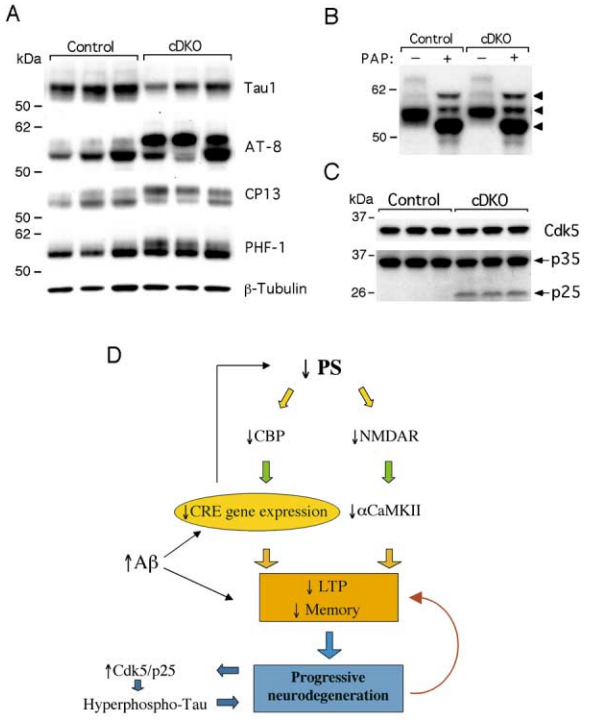

Figure 8. Hyperphosphorylation of Tau and Increased Levels of p25 in Aged *PS* cDKO Mice

(A) Hyperphosphorylation of tau in the *PS* cDKO cerebral cortex at 9 months of age. Western analysis shows decreased immunoreactivity with Tau-1 antibody, which recognizes dephosphorylated residues Ser202/Thr205, and increased phosphorylation at Ser202/Thr205 (AT-8), Ser202 (CP13), and Ser396/404 (PHF-1) in cortical lysates from *PS* cDKO mice.

(B) Western analysis of cortical lysates treated (+) or untreated (−) with potato acid phosphatase (PAP) shows similar levels of tau isoforms (arrowheads) recognized by Tau-1 antibodies in *PS* cDKO and control mice.

(C) Normal levels of Cdk5 and p35 but increased levels of p25 in *PS* cDKO brains at 9 months of age.

(D) A model depicting molecular pathways regulated by presenilins leading to impaired synaptic plasticity and memory followed by neurodegeneration.

crucial roles in these processes. We first addressed the function of NMDARs, which are required for the induction of LTP and the formation of long-term memory (Bliss and Collingridge, 1993). Moreover, conditional inactivation of the NR1 subunit in hippocampal area CA1 has been shown to cause prominent defects in Schaeffer collateral LTP and spatial memory (Tsien et al., 1996). Although synaptic transmission and AMPAR-dependent synaptic responses were normal at CA1 synapses in *PS* cDKO mice, NMDAR-dependent responses were significantly reduced. We detected a parallel reduction in the synaptic levels of NMDAR subunits (NR1 and NR2A), providing a likely molecular basis for the observed impairment of synaptic NMDAR activity. In contrast, total cellular levels of NMDARs were normal in *PS* cDKO mice, suggesting that the selective reduction in synaptic NMDAR levels may be due to a defect in intracellular trafficking or synaptic delivery. Consistent with this view, we detected a specific physical interaction between PS1 and NMDARs in cerebral cortical lysates, suggesting that PS1 forms a stable complex with NMDARs that facilitates their proper synaptic delivery or localization. Previous evidence implicating PS1 in the trafficking of other synaptic transmembrane proteins, including TrkB and cadherins (Naruse et al., 1998; Uemura et al., 2003), provides further support for such a mechanism.

CaMKII is a primary downstream effector of NMDARs in LTP induction, and recent work has demonstrated physical and functional interactions between NMDARs and CaMKII. NMDAR stimulation elicits the translocation of CaMKII to postsynaptic sites, where CaMKII is activated by NMDAR-triggered calcium influx (Lisman et al., 2002). In addition, neuronal levels of the α and β isoforms of CaMKII are inversely regulated by synaptic activity, with levels of αCaMKII increasing in response to NMDAR-dependent activity and levels of βCaMKII increasing in response to AMPAR blockade (Thiagarajan et al., 2002). Since mRNA for the αCaMKII isoform is present in dendrites, while mRNA for the β isoform is absent, local translation in response to NMDAR activity has been proposed to regulate synaptodendritic levels of αCaMKII (Steward and Schuman, 2001). The functional significance of the dendritic localization of αCaMKII mRNA is supported by the recent finding that genetic ablation of the subset of αCaMKII mRNA localized to dendrites caused deficits in LTP and spatial and contextual memory (Miller et al., 2002). In *PS* cDKO mice, we observed a selective reduction in both synaptic and dendritic αCaMKII, while total αCaMKII levels, as well as total and synaptic levels of βCaMKII and CaMKIV, appeared normal. In view of the important role of NMDARs in determining both the synaptic localization and the levels of αCaMKII, the reduction in synaptodendritic αCaMKII may be a direct consequence of the decreased synaptic levels and activity of NMDARs in *PS* cDKO mice.

CRE-dependent gene expression has been demonstrated to play an important role in the consolidation of long-term forms of synaptic plasticity and memory (Silva et al., 1998). In our study, we found a consistent reduction in the expression of multiple CREB/CBP target genes, including *c-fos* and *BDNF*, in the *PS* cDKO cerebral cortex. Although nuclear levels of CREB and Ser133-phosphorylated CREB were normal in the *PS* cDKO cerebral cortex, levels of CBP mRNA and protein were significantly decreased. Since CBP is an essential cofactor for transcriptional activation by CREB, diminished CBP expression represents the likely basis for the global reduction in the transcription of CRE-bearing genes. Our identification of a previously unrecognized consensus CBF-1 binding site in the *CBP* proximal promoter in turn suggests that the observed reduction in *CBP* transcription is a consequence of impaired Notch signaling in the absence of PS. The dependence of Notch signaling activity on PS, which participate in the proteolytic cleavage of Notch to generate the constitutively active intracellular domain (NICD), has been well documented. Upon proteolytic release, NICD translocates to the nucleus and associates with the sequence-specific DNA binding factor CBF-1 to activate transcription of responsive genes. Thus, our findings suggest a cascade in which PS-dependent Notch signaling indirectly regulates CRE-dependent gene expression through the regulation of Notch-dependent CBP expression.

The global reduction in CRE-dependent gene expression caused by loss of PS function in our study is in direct disagreement with a recent study reporting increased expression of *c-fos* as a consequence of PS1 inactivation (Marambaud et al., 2003). In this report, reduced N-cadherin processing in cultured *PS1* null cells was found to cause decreased cytoplasmic retention of CBP and increased *c-fos* expression. In contrast, we examined the expression of multiple CRE-dependent genes, including *c-fos*, by quantitative methods in the adult cerebral cortex, and we identified a consistent reduction in CRE-dependent transcription in the absence of PS function. Moreover, we also identified a parallel reduction in both nuclear and cytoplasmic CBP levels as a consequence of PS inactivation, providing a mechanism for the reduced transcription of CRE-dependent genes. While the basis for the discrepancy between the two studies is unclear, it may reflect differences in methodology (e.g., RT-PCR versus quantitative real-time RT-PCR) or experimental system (i.e., cell culture versus adult brain).

Essential Role of Presenilins in Neuronal Survival

In the present study, loss of PS function was sufficient to cause progressive, age-dependent neurodegeneration, demonstrating that PS are essential for neuronal survival in the adult brain. Synaptic and neuronal loss in *PS* cDKO mice are preceded by defects in LTP and its underlying molecular mechanisms, raising the possibility that impairments in synaptic plasticity may lead over time to structural deterioration and death of neurons. Indeed, LTP is thought to promote stabilization and growth of synaptic connections, primarily through the induction of new mRNA and protein synthesis (Kandel, 2001). In addition to its important role in synaptic plasticity, CRE-dependent gene expression appears to play an important role in neuronal survival (Walton and Dragunow, 2000). Conditional inactivation of CREB and CREM in the adult forebrain causes age-dependent neurodegeneration (Mantamadiotis et al., 2002). Moreover, reduced CBP function and reduced CRE-dependent gene expression have been implicated in the pathogenesis of neurodegeneration in polyglutamine repeat disorders (Nucifora et al., 2001). Thus, the reductions in CBP levels and CRE-dependent gene expression in *PS* cDKO cerebral cortex, which are evident prior to the onset of detectable neuropathological changes, likely contribute to the subsequent neuronal degeneration. These observations suggest that downregulation of CRE-dependent gene expression may constitute a common pathway leading to impaired synaptic plasticity and subsequent neurodegeneration. Expression of BDNF, which is a potent regulator of both LTP and neuronal survival, is induced by NMDAR activity in a CRE-dependent manner, providing one candidate mechanism for mediation of this dual effect.

A growing body of evidence has established an important role for the cytoskeletal protein tau in neuronal survival. Accumulation of hyperphosphorylated tau characterizes the neurodegeneration in both AD and FTD. Recent work has demonstrated excessive activation of Cdk5 in the AD brain as a consequence of increased cleavage of its activator p35 to generate the more potent activator p25 (Patrick et al., 1999). Interestingly, increased levels of p25 and tau hyperphosphorylation accompanied neurodegeneration in the cerebral cortex of *PS* cDKO mice. Consistent with p25-induced Cdk5 activation, excessive phosphorylation of tau occurred on multiple residues known to be phosphorylated in vivo by Cdk5. These observations suggest that loss of PS function can precipitate dysfunction of Cdk5 and tau, which may further contribute to the progressive neurodegeneration in *PS* cDKO mice.

On the basis of our findings, we propose a model in which loss of PS function in the adult brain causes neurodegeneration via two primary mechanisms (Figure 8D). First, PS inactivation impairs the central mechanisms underlying synaptic plasticity, most significantly NMDAR function and CREB/CBP-dependent gene expression, and these defects then promote subsequent neurodegeneration. Second, PS inactivation leads to inappropriate activation of Cdk5 and tau hyperphosphorylation at later ages, which then exacerbate the ongoing neurodegeneration.

Pathogenic Mechanism Underlying PS Mutations: Gain of Function and/or Loss of Function?

FAD-linked PS mutations generally cause a selective enhancement of the production of Aβ42 peptides, though total Aβ production is often unchanged or reduced. This increase in the more fibrillogenic form of Aβ has led to the prevailing view that PS mutations cause FAD through a toxic, gain-of-function mechanism. However, accumulating evidence also suggests a partial loss-of-function pathogenic mechanism. First, PS mutations are generally associated with a more aggressive course and earlier onset of FAD than is the case with APP mutations, even though APP mutations lead to higher levels of Aβ42 and/or total Aβ production. Thus, the increased Aβ42 production induced by PS mutations alone may not explain the greater severity of PS-linked FAD, suggesting that PS mutations exert additional pathogenic effects. Second, the identification of exonic deletion mutations in PS1 and very large numbers of distinct missense mutations distributed throughout the coding sequence in PS-linked FAD pedigrees is more consistent with a partial loss-of-function than a toxic gain-of-function pathogenic mechanism. Third, genetic studies in *C. elegans* (Baumeister et al., 1997; Levitan et al., 1996; Lewis et al., 2000) have ascribed reduced activities to presenilin homologs bearing FAD-associated mutations. Fourth, recent biochemical studies have documented that a variety of FAD-linked PS mutations confer reductions in γ-secretase-dependent cleavages of Notch and APP to generate NICD and AICD, respectively (Moehlmann et al., 2002; Schroeter et al., 2003; Song et al., 1999). Finally, a pathogenic PS1 mutation essentially devoid of γ-secretase activity has recently been reported (Amtul et al., 2002), and a polymorphism in the *PS1* promoter, which decreases PS1 expression, constitutes a risk factor for sporadic AD (Theuns et al., 2003).

Our findings of memory impairment and age-dependent neurodegeneration in *PS* cDKO mice provide further support for a previously unappreciated contribution of loss of PS function to the pathogenesis of FAD. Though complete loss of PS function, which would likely

result in embryonic lethality, is not found in FAD, partial loss of PS function may nonetheless cause similar memory impairments and progressive neurodegeneration over a more protracted time scale. In addition, there is some evidence that PS bearing FAD-linked mutations possess dominant-negative activity, thereby impairing the function of PS derived from normal alleles (Schroeter et al., 2003). Moreover, *PS1* is itself a CREB/CBP target gene whose expression can be induced by NMDAR activity and BDNF (Mitsuda et al., 2001). Our findings therefore imply that partial loss of PS function may be compounded by a consequent reduction in *PS1* transcription.

Our results suggest that impairments in synaptic plasticity and CRE-dependent gene expression may be early pathogenic events that promote the subsequent development of neurodegeneration. Since FAD-linked PS mutations with diminished γ-secretase activity can nonetheless enhance Aβ42 production, the deleterious effects of Aβ on neuronal physiology and survival (Kamenetz et al., 2003; Yankner et al., 1989) may further contribute to neurodegeneration associated with reduced PS function. Excessive levels of Aβ peptides have also been reported to cause cellular and molecular deficits similar to those identified in our study, including impairments in synaptic plasticity and memory (Hsia et al., 1999; Hsiao et al., 1996) and CRE-dependent gene expression (Tong et al., 2001; Vitolo et al., 2002). Thus, partial loss of PS function and elevated Aβ levels may cooperate to reduce CRE-dependent gene expression, which may in turn downregulate expression of the normal *PS1* allele (Figure 8D). Indeed, it has been reported that PS1 expression is selectively reduced in the association neocortex and hippocampus of AD brains (Davidsson et al., 2001). We would therefore propose that Aβ-dependent pathogenic effects act in concert with partial loss of presenilin function to cause memory loss and neurodegeneration in FAD.

In summary, *PS* cDKO mice provide a valuable model system for dissection of the early events and molecular pathways leading to neurodegeneration in AD. The molecular mechanisms by which reduced PS function leads to impaired synaptic function and neuronal survival may offer new targets for therapeutic intervention. Finally, these findings raise the valid concern that inhibition of presenilin function may accelerate, rather than attenuate, the development of memory loss and neurodegeneration, and thus call for caution in the use of γ-secretase inhibitors as a therapeutic strategy in Alzheimer's disease.

Experimental Procedures

Mice

The generation of *PS1* cKO and *PS2*$^{-/-}$ were described previously (Steiner et al., 1999; Yu et al., 2001). *PS* cDKO mice were generated by crossing *PS1* cKO (*fPS1/fPS1;*α*CaM-Cre*) with *PS2*$^{-/-}$ mice. All four experimental genotypic groups (*fPS1/fPS1;*α*CaM-Cre;PS2*−/−, *fPS1/fPS1;* α*CaM-Cre*, *fPS1/fPS1;PS2*−/−, and *fPS1/fPS1*) were obtained from two crosses (*fPS1/fPS1;PS2*−/−;α*CaM-Cre* × *fPS1/fPS1;PS2*−/− and *fPS1/fPS1;* α*CaM-Cre* × *fPS1/fPS1*), and littermates were used for all experiments. *fPS1/fPS1* and *PS2*$^{-/-}$ mice were generated in C57BL6/129 hybrid background, whereas α*CaM*-Cre transgenic mice were generated in C57BL6/CBA hybrid strain and then backcrossed to B6 for more than 10 generations. Therefore, the genetic background of all experimental groups was C57BL6/129 hybrid. The experimenters of behavioral, electrophysiological, and morphological studies were blind to the genotypes of the mice.

Histology

Paraffin-embedded sagittal brain sections (10 μm) were immunostained with monoclonal antibodies raised against MAP2 (1:200; Sigma), synaptophysin (1:200; Sigma), GFAP (1:500; Sigma), or αCaMKII (Santa Cruz; 1:750), incubated with either Alexa Fluor 488 or 594 anti-mouse secondary antibodies (Molecular Probes), and then analyzed with a Zeiss 510 confocal laser scanning microscope. Neuron counts were performed using the optical dissector technique as described (Irizarry et al., 1997). Golgi staining and dendritic quantifications were performed as described (Vyas et al., 2002).

Behavioral Tests

The water maze is a circular pool 160 cm in diameter. Each mouse was given 6 trials daily (2 trials per block, ~2 hr interblock interval) for 5 days. The movement of the mice was monitored using an automated tracking system (HVS Image). Following training days 3 and 5, mice were subjected to a 60 s probe trial in which the platform was removed and the mice were allowed to search for it. In the visible platform test, extramaze distal cues were removed, and the platform was raised above water and marked by a black and white golf ball.

For contextual fear conditioning, on training day, mice were placed within the conditioning chamber for 3 min before the onset of the footshock. Following a 1 s/1 mA single footshock, they were allowed to remain in the chamber for an additional 2 min and then returned to their home cages. Mice were tested 24 hr following training for 4 min in the same conditioning chamber. Freezing was defined as a complete cessation of movement except for respiration and scored by an automated system (Actimetrics).

Electrophysiology

Acute hippocampal slices (400 μm) were maintained in a storage chamber containing artificial cerebrospinal fluid (aCSF: 124 mM NaCl, 5 mM KCl, 1.25 mM NaH_2PO_4, 3 mM $MgCl_2$, 1 mM $CaCl_2$, 26 mM $NaHCO_3$, 10 mM dextrose [pH 7.4]) at 30°C as described (Yu et al., 2001). Stimulation (200 μs) pulses were delivered with a bipolar concentric metal electrode. Synaptic strength was quantified as the initial slope of field potentials recorded with aCSF-filled microelectrodes (1 to 2 MΩ). Baseline responses were collected at 0.07 Hz with a stimulation intensity that yielded a half-maximal response. LTP was induced by five episodes of TBS delivered at 0.1 Hz. Each episode contains ten stimulus trains (4 pulses at 100 Hz) delivered at 5 Hz. Average responses (mean ± SEM) are expressed as percent of pre-TBS baseline response. LTD was induced with 900 paired-pulses (40 ms apart) delivered at 1 Hz. NMDAR responses were recorded in the presence of 10 μM CNQX and 10 μM BMI to block AMPAR and GABA type A receptor-mediated responses, respectively. Repeated measures ANOVA and nonpaired t test were used to assess statistical significance.

Whole-cell recordings were performed in CA1 pyramidal neurons visually identified with an IR-DIC Zeiss microscope. Patch pipettes (2–4 MΩ) were filled with internal solution consisting of (in mM): 130 CsGluconate, 8 KCl, 10 EGTA, 10 HEPES, 5 QX-314, 3 ATP, 0.3 GTP (pH 7.4); 275–285 mOsm. The junction potential (less than 5 mV) was not compensated. Only neurons with membrane potentials greater than −65 mV and input resistance greater than 70 MΩ (103.17 ± 4.48 MΩ) were studied. NMDAR-dependent and AMPAR-dependent responses were discriminated based on their distinct kinetics and voltage dependence: the NMDAR-mediated currents were measured at +40 mV, 100 ms after the response onset, whereas the AMPAR-mediated currents were taken as the peak amplitude response recorded at −80 mV.

Preparation of Synaptoneurosomes, Immunoprecipitation, and Western Analysis

Synaptoneurosomes were prepared from adult cerebral cortex essentially as described (Scheetz et al., 2000). For the detection of Tau, cortices were homogenized in cold buffer (62.5 mM Tris HCl

[pH 6.8], 10% glycerol, 5% 2-mercaptoethanol, 2.3% SDS, 1 mM EDTA, 1 mM EGTA, protease and phosphatase inhibitors) and boiled at 100°C for 5 min. For dephosphorylation assays, lysates were incubated in 10 mM PIPES (pH 6.0) at 37°C for 20 min in the presence or absence of potato acid phosphatase (0.02 units/ml). For immunoprecipitation assays, cortical membranes were solubilized in IP buffer (25 mM HEPES [pH 7.4], 150 mM NaCl, 2 mM EDTA, 1% NP40, and protease inhibitors). The lysates were incubated with an anti-PS1 antibody (B19.2) or rabbit serum and protein A-Sepharose. The immunocomplexes were washed and analyzed by SDS-PAGE. For Western analysis, same amounts of protein were resolved on SDS-PAGE and developed using the ECL chemiluminiscence kit (NEN) or ^{125}I-labeled secondary antibodies (ICN Biomedicals) as previously described (Yu et al., 2001). Protein levels were quantified using a phosphorimager (Molecular Dynamics) and normalized to β-actin (Abcam) or lamin B_1 (Zymed).

Quantitative Real-Time RT-PCR

Total cortical RNA (1 μg) was treated with DNase I and reverse transcribed using the SuperScript First-Strand Synthesis kit (Invitrogen) in the presence of random hexamers. PCR reactions were performed in a total volume of 30 μl using SYBR Green PCR mastermix in an ABI PRISM 7700 Sequence Detector (Applied Biosystems), using 10 μl of diluted (1:25) cDNA and gene-specific primers. Amplification was performed using the following conditions: 50°C for 2 min, 95°C for 10 min, and 40 cycles of 95°C for 15 s and 60°C for 1 min. Reactions were performed in duplicates, and threshold cycle (Ct) values were normalized to 18S RNA. All procedures were carried out together for *PS* cDKO and control in gender-matched pairs. The PCR products were separated by electrophoresis to confirm their correct product size.

Acknowledgments

We thank P. Davis for CP13 and PHF-1 and B. De Strooper for B19.2 antibodies; R. Kopan, M. Feany, L.-H. Tsai, B. Alger, and members of our laboratory for helpful discussions; W. Cheng, S. Lincoln, A. Martins, and W. Wang for assistance; and M. Irizarry for advice on the stereological counting method. The work was supported by grants from the Alzheimer's Association (C.A.S., J.S.) and the NINDS (NS41783 to J.S.). E.R.K. is one of four founders of Memory Pharmaceuticals and Chairman of its Scientific Advisory Board. Memory Pharmaceuticals is concerned with developing drugs for age-related memory loss. Some of these drugs are also potentially useful in depression and schizophrenia.

Received: January 7, 2003
Revised: December 23, 2003
Accepted: March 9, 2004
Published online: April 1, 2004

References

Amtul, Z., Lewis, P.A., Piper, S., Crook, R., Baker, M., Findlay, K., Singleton, A., Hogg, M., Younkin, L., Younkin, S.G., et al. (2002). A presenilin 1 mutation associated with familial frontotemporal dementia inhibits γ-secretase cleavage of APP and Notch. Neurobiol. Dis. *9*, 269–273.

Baumeister, R., Leimer, U., Zweckbronner, I., Jakubek, C., Grunberg, J., and Haass, C. (1997). Human presenilin-1, but not familial Alzheimer's disease (FAD) mutants, facilitate *Caenorhabditis elegans* notch signalling independently of proteolytic processing. Genes Funct. *1*, 149–159.

Bliss, T., and Collingridge, G. (1993). A synaptic model of memory: long-term potentiation in the hippocampus. Nature *361*, 31–39.

Braak, E., and Braak, H. (1997). Alzheimer's disease: transiently developing dendritic changes in pyramidal cells of sector CA1 of the Ammon's horn. Acta Neuropathol. (Berl.) *93*, 323–325.

Cao, X., and Sudhof, T.C. (2001). A transcriptionally active complex of APP with Fe65 and histone acetyltransferase Tip60. Science *293*, 115–120.

Crook, R., Verkkoniemi, A., Perez-Tur, J., Mehta, N., Baker, M., Houlden, H., Farrer, M., Hutton, M., Lincoln, S., Hardy, J., et al. (1998). A variant of Alzheimer's disease with spastic paraparesis and unusual plaques due to deletion of exon 9 of presenilin 1. Nat. Med. *4*, 452–455.

Davidsson, P., Bogdanovic, N., Lannfelt, L., and Blennow, K. (2001). Reduced expression of amyloid precursor protein, presenilin-1 and rab3a in cortical brain regions in Alzheimer's disease. Dement. Geriatr. Cogn. Disord. *12*, 243–250.

De Strooper, B., Saftig, P., Craessaerts, K., Vanderstichele, H., Guhde, G., Annaert, W., Von Figura, K., and Van Leuven, F. (1998). Deficiency of presenilin-1 inhibits the normal cleavage of amyloid precursor protein. Nature *391*, 387–390.

De Strooper, B., Annaert, W., Cupers, P., Saftig, P., Craessaerts, K., Mumm, J.S., Schroeter, E.H., Schrijvers, V., Wolfe, M.S., Ray, W.J., et al. (1999). A presenilin-1-dependent γ-secretase-like protease mediates release of Notch intracellular domain. Nature *398*, 518–522.

Donoviel, D.B., Hadjantonakis, A., Ikeda, M., Zheng, H., St George Hyslop, P., and Bernstein, A. (1999). Mice lacking both presenilin genes exhibit early embryonic patterning defects. Genes Dev. *13*, 2801–2810.

Fleischmann, A., Hvalby, O., Jensen, V., Strekalova, T., Zacher, C., Layer, L.E., Kvello, A., Reschke, M., Spanagel, R., Sprengel, R., et al. (2003). Impaired long-term memory and NR2A-type NMDA receptor-dependent synaptic plasticity in mice lacking c-Fos in the CNS. J. Neurosci. *23*, 9116–9122.

Handler, M., Yang, X., and Shen, J. (2000). Presenilin-1 regulates neuronal differentiation during neurogenesis. Development *127*, 2593–2606.

Hsia, A.Y., Masliah, E., McConlogue, L., Yu, G.Q., Tatsuno, G., Hu, K., Kholodenko, D., Malenka, R.C., Nicoll, R.A., and Mucke, L. (1999). Plaque-independent disruption of neural circuits in Alzheimer's disease mouse models. Proc. Natl. Acad. Sci. USA *96*, 3228–3233.

Hsiao, K., Chapman, P., Nilsen, S., Ekman, C., Harigaya, Y., Younkin, S., Yang, F., and Cole, G. (1996). Correlative memory deficits, Aβ elevation, and amyloid plaques in transgenic mice. Science *274*, 99–102.

Hutton, M., and Hardy, J. (1997). The presenilins and Alzheimer's disease. Hum. Mol. Genet. *6*, 1639–1646.

Irizarry, M., McNamara, M., Fedorchak, K., Hsiao, K., and Hyman, B. (1997). APPsw transgenic mice develop age-related Aβ deposits and neuropil abnormalities but not neuronal loss in CA1. J. Neuropathol. Exp. Neurol. *56*, 173–177.

Kamenetz, F., Tomita, T., Hsieh, H., Seabrook, G., Borchelt, D., Iwatsubo, T., Sisodia, S., and Malinow, R. (2003). APP processing and synaptic function. Neuron *37*, 925–937.

Kandel, E.R. (2001). The molecular biology of memory storage: a dialogue between genes and synapses. Science *294*, 1030–1038.

Kemp, N., and Bashir, Z. (1997). NMDA receptor-dependent and -independent long-term depression in the CA1 region of the adult rat hippocampus in vitro. Neuropharmacology *36*, 397–399.

Korte, M., Carroll, P., Wolf, E., Brem, G., Thoenen, H., and Bonhoeffer, T. (1995). Hippocampal long-term potentiation is impaired in mice lacking brain-derived neurotrophic factor. Proc. Natl. Acad. Sci. USA *92*, 8856–8860.

Levitan, D., Doyle, T.G., Brousseau, D., Lee, M.K., Thinakaran, G., Slunt, H.H., Sisodia, S.S., and Greenwald, I. (1996). Assessment of normal and mutant human presenilin function in *Caenorhabditis elegans*. Proc. Natl. Acad. Sci. USA *93*, 14940–14944.

Lewis, P.A., Perez-Tur, J., Golde, T.E., and Hardy, J. (2000). The presenilin 1 C92S mutation increases abeta 42 production. Biochem. Biophys. Res. Commun. *277*, 261–263.

Lisman, J., Schulman, H., and Cline, H. (2002). The molecular basis of CaMKII function in synaptic and behavioural memory. Nat. Rev. Neurosci. *3*, 175–190.

Lonze, B.E., and Ginty, D.D. (2002). Function and regulation of CREB family transcription factors in the nervous system. Neuron *35*, 605–623.

Mantamadiotis, T., Lemberger, T., Bleckmann, S., Kern, H., Kretz,

O., Villalba, A., Tronche, F., Kellendonk, C., Gau, D., Kapfhammer, J., et al. (2002). Disruption of CREB function in brain leads to neurodegeneration. Nat. Genet. *31*, 47–54.

Marambaud, P., Wen, P.H., Dutt, A., Shioi, J., Takashima, A., Siman, R., and Robakis, N.K. (2003). A CBP binding transcriptional repressor produced by the PS1/ϵ-cleavage of N-cadherin is inhibited by PS1 FAD mutations. Cell *114*, 635–645.

Miller, S., Yasuda, M., Coats, J.K., Jones, Y., Martone, M.E., and Mayford, M. (2002). Disruption of dendritic translation of CaMKIIα impairs stabilization of synaptic plasticity and memory consolidation. Neuron *36*, 507–519.

Mitsuda, N., Ohkubo, N., Tamatani, M., Lee, Y., Taniguchi, M., Namikawa, K., Kiyama, H., Yamaguchi, A., Sato, N., Sakata, K., et al. (2001). Activated cAMP-response element-binding protein regulates neuronal expression of presenilin-1. J. Biol. Chem. *276*, 9688–9698.

Moehlmann, T., Winkler, E., Xia, X., Edbauer, D., Murrell, J., Capell, A., Kaether, C., Zheng, H., Ghetti, B., Haass, C., and Steiner, H. (2002). Presenilin-1 mutations of leucine 166 equally affect the generation of the Notch and APP intracellular domains independent of their effect on Aβ 42 production. Proc. Natl. Acad. Sci. USA *99*, 8025–8030.

Naruse, S., Thinakaran, G., Luo, J.J., Kusiak, J.W., Tomita, T., Iwatsubo, T., Qian, X., Ginty, D.D., Price, D.L., Borchelt, D.R., et al. (1998). Effects of PS1 deficiency on membrane protein trafficking in neurons. Neuron *21*, 1213–1221.

Nucifora, F.C., Jr., Sasaki, M., Peters, M.F., Huang, H., Cooper, J.K., Yamada, M., Takahashi, H., Tsuji, S., Troncoso, J., Dawson, V.L., et al. (2001). Interference by huntingtin and atrophin-1 with CBP-mediated transcription leading to cellular toxicity. Science *291*, 2423–2428.

Patrick, G.N., Zukerberg, L., Nikolic, M., de la Monte, S., Dikkes, P., and Tsai, L.-H. (1999). Conversion of p35 to p25 deregulates Cdk5 activity and promotes neurodegeneration. Nature *402*, 615–622.

Patterson, S.L., Abel, T., Deuel, T.A., Martin, K.C., Rose, J.C., and Kandel, E.R. (1996). Recombinant BDNF rescues deficits in basal synaptic transmission and hippocampal LTP in BDNF knockout mice. Neuron *16*, 1137–1145.

Scheetz, A.J., Nairn, A.C., and Constantine-Paton, M. (2000). NMDA receptor-mediated control of protein synthesis at developing synapses. Nat. Neurosci. *3*, 211–216.

Schroeter, E.H., Ilagan, M.X., Brunkan, A.L., Hecimovic, S., Li, Y.M., Xu, M., Lewis, H.D., Saxena, M.T., De Strooper, B., Coonrod, A., et al. (2003). A presenilin dimer at the core of the γ-secretase enzyme: insights from parallel analysis of Notch 1 and APP proteolysis. Proc. Natl. Acad. Sci. USA *100*, 13075–13080.

Shen, J., Bronson, R.T., Chen, D.F., Xia, W., Selkoe, D.J., and Tonegawa, S. (1997). Skeletal and CNS defects in presenilin-1 deficient mice. Cell *89*, 629–639.

Silva, A.J., Kogan, J.H., Frankland, P.W., and Kida, S. (1998). CREB and memory. Annu. Rev. Neurosci. *21*, 127–148.

Song, W., Nadeau, P., Yuan, M., Yang, X., Shen, J., and Yankner, B.A. (1999). Proteolytic release and nuclear translocation of Notch-1 are induced by presenilin-1 and impaired by pathogenic presenilin-1 mutations. Proc. Natl. Acad. Sci. USA *96*, 6959–6963.

Steiner, H., Duff, K., Capell, A., Romig, H., Grim, M.G., Lincoln, S., Hardy, J., Yu, X., Picciano, M., Fechteler, K., et al. (1999). A loss of function mutation of presenilin-2 interferes with amyloid β-peptide production and Notch signaling. J. Biol. Chem. *274*, 28669–28673.

Steward, O., and Schuman, E.M. (2001). Protein synthesis at synaptic sites on dendrites. Annu. Rev. Neurosci. *24*, 299–325.

Tao, X., Finkbeiner, S., Arnold, D.B., Shaywitz, A.J., and Greenberg, M.E. (1998). Ca^{2+} influx regulates BDNF transcription by a CREB family transcription factor-dependent mechanism. Neuron *20*, 709–726.

Terry, R.D., Masliah, E., Salmon, D.P., Butters, N., DeTeresa, R., Hill, R., Hansen, L.A., and Katzman, R. (1991). Physical basis of cognitive alterations in Alzheimer's disease: synapse loss is the major correlate of cognitive impairment. Ann. Neurol. *30*, 572–580.

Theuns, J., Remacle, J., Killick, R., Corsmit, E., Vennekens, K., Huyle-broeck, D., Cruts, M., and Van Broeckhoven, C. (2003). Alzheimer-associated C allele of the promoter polymorphism -22C>T causes a critical neuron-specific decrease of presenilin 1 expression. Hum. Mol. Genet. *12*, 869–877.

Thiagarajan, T.C., Piedras-Renteria, E.S., and Tsien, R.W. (2002). α- and β-CaMKII. Inverse regulation by neuronal activity and opposing effects on synaptic strength. Neuron *36*, 1103–1114.

Tong, L., Thornton, P.L., Balazs, R., and Cotman, C.W. (2001). Beta-amyloid-(1–42) impairs activity-dependent cAMP-response element-binding protein signaling in neurons at concentrations in which cell survival is not compromised. J. Biol. Chem. *276*, 17301–17306.

Tsien, J.Z., Huerta, P.T., and Tonegawa, S. (1996). The essential role of hippocampal CA1 NMDA receptor-dependent synaptic plasticity in spatial memory. Cell *87*, 1327–1338.

Tysoe, C., Whittaker, J., Xuereb, J., Cairns, N., Cruts, M., Van Broeckhoven, C., Wilcock, G., and Rubinsztein, D. (1998). A presenilin-1 truncating mutation is present in two cases with autopsy-confirmed early-onset Alzheimer disease. Am. J. Hum. Genet. *62*, 70–76.

Uemura, K., Kitagawa, N., Kohno, R., Kuzuya, A., Kageyama, T., Chonabayashi, K., Shibasaki, H., and Shimohama, S. (2003). Presenilin 1 is involved in maturation and trafficking of N-cadherin to the plasma membrane. J. Neurosci. Res. *74*, 184–191.

Vitolo, O.V., Sant'Angelo, A., Costanzo, V., Battaglia, F., Arancio, O., and Shelanski, M. (2002). Amyloid beta -peptide inhibition of the PKA/CREB pathway and long-term potentiation: reversibility by drugs that enhance cAMP signaling. Proc. Natl. Acad. Sci. USA *99*, 13217–13221.

Vyas, A., Mitra, R., Shankaranarayana Rao, B., and Chattarji, S. (2002). Chronic stress induces contrasting patterns of dendritic remodeling in hippocampal and amygdaloid neurons. J. Neurosci. *22*, 6810–6818.

Walton, M.R., and Dragunow, I. (2000). Is CREB a key to neuronal survival? Trends Neurosci. *23*, 48–53.

Yankner, B.A., Dawes, L.R., Fisher, S., Villa-Komaroff, L., Oster-Granite, M.L., and Neve, R.L. (1989). Neurotoxicity of a fragment of the amyloid precursor associated with Alzheimer's disease. Science *245*, 417–420.

Yu, H., Saura, C.A., Choi, S.-Y., Sun, L.D., Yang, X., Handler, M., Kawarabayashi, T., Younkin, L., Fedeles, B., Wilson, M.A., et al. (2001). APP processing and synaptic plasticity in Presenilin-1 conditional knockout mice. Neuron *31*, 713–726.